MOLECULAR AND CELLULAR BIOLOGY, Dec. 1982, p. 1581–1594
0270-7306/82/121581-14$02.00/0

Vol. 2, No. 12

Kinetics of Accumulation and Processing of Simian Virus 40 RNA in *Xenopus laevis* Oocytes Injected with Simian Virus 40 DNA

TIMOTHY J. MILLER,† DONALD L. STEPHENS, AND JANET E. MERTZ*

McArdle Laboratory for Cancer Research, University of Wisconsin, Madison, Wisconsin 53706

Received 28 July 1982/Accepted 21 September 1982

We examined the kinetics of accumulation and processing of simian virus 40 (SV40) RNA in stage 6 oocytes of *Xenopus laevis* microinjected intranuclearly with SV40 DNA. The rates of synthesis and degradation, cellular distribution, size, and sequence specificity of radiolabeled SV40-specific and endogenous oocyte RNA were determined. The kinetics of accumulation of SV40 RNA were biphasic, with greater than 90% of the viral RNA turning over in the nucleus with a half-life of 20 to 40 min. Although most of the primary transcription products were multigenomic in length, some stable polyadenylated SV40-specific RNA similar in size and sequence to late 19S mRNA accumulated in the cytoplasm with time. Differences in strand preference, efficiencies of transcription termination and polyadenylation, and the splice sites used in the synthesis and processing of SV40 RNA in *Xenopus* oocytes and monkey cells were noted. However, these differences were quantitative, rather than qualitative, in nature. Consequently, they are probably due to regulatory rather than mechanistic differences between the two cell types. We therefore conclude that *Xenopus* oocytes may be a useful system for studying both mechanistic and cell type-specific regulatory aspects of mRNA biogenesis from cloned DNAs. However, since only a small percentage of the initially synthesized RNA ends up in stable mRNA, it will be important to determine whether mutants of cloned DNAs that produce abnormal amounts of stable mRNAs are altered in promotion and initiation of RNA synthesis, transcription termination, RNA processing, or the stability of the resultant mRNAs.

Anderson and Smith (3) have studied the synthesis and degradation of heterogeneous nuclear RNA in stage 6 oocytes of *Xenopus laevis*. Their data indicate that approximately 95% of this RNA turns over in the nucleus and that it possesses many of the characteristics seen for heterogeneous nuclear RNA made in somatic cells. However, it would be useful to follow the synthesis of specific mRNAs rather than the heterogeneous mixture of all mRNAs made by oocytes. Mertz and Gurdon (24) discovered that purified DNAs from heterologous sources are transcriptionally active after microinjection into the nucleus (germinal vesicle) of *Xenopus* oocytes. Since then, numerous workers have demonstrated that a variety of genes encoding proteins, as well as tRNAs and 5S RNA from both homologous and heterologous species, are transcribed faithfully in *Xenopus* oocytes by the appropriate RNA polymerases (6, 9, 10, 15, 19, 20, 22, 26, 31; see ref. 16 for review). Consequently, the *Xenopus* oocyte system may be useful for examining various mechanistic details concerned with expression of cloned eucaryotic genes.

We have studied transcription of simian virus 40 (SV40) DNA, a small double-stranded DNA virus whose natural host is monkeys. Although SV40 DNA is not normally expressed in frog cells, we decided to use this small, 5,243-base-pair genome for several reasons. First of all, the SV40 genome is one of the best characterized eucaryotic DNAs (see ref. 36 for review). It is almost completely dependent upon the host for its expression and uses cellular enzymes for synthesizing and processing its RNAs. Its DNA is found in association with cellular chromosomal proteins in the usual nucleosomal arrangement, and this viral "minichromosome" is transcribed by RNA polymerase II. In addition, there exist both early and late phases to the expression of its genome during its normal lytic

† Present address: Norden Laboratory, Lincoln, NE 68521.

cycle of infection of monkey cells. Finally, the SV40-encoded proteins are known to be synthesized in SV40 DNA-injected oocytes (9, 13a, 31). Therefore, at least some of the virus-specific RNA is properly processed, transported, and translated. Thus, SV40 can not only be used to study promotion and initiation by RNA polymerase II, but also to examine various aspects of RNA processing and transport, translation, and post-translational modification of proteins.

In this paper, we analyze the kinetics of accumulation and processing of SV40-specific RNA in *Xenopus* oocytes and show that, as expected for mRNAs, some of the virus-specific RNA becomes polyadenylated [poly(A)$^+$], and a small percentage of it is transported to the cytoplasm where it gradually accumulates as a set of species similar in size and sequence to those seen in infected monkey cells. The information presented here should be useful to anyone employing the *Xenopus* oocyte system for studying the expression of cloned eucaryotic message-encoding DNAs. Furthermore, it reminds us of the importance when mapping promoters of determining whether mutants of cloned DNAs that produce abnormal amounts of stable mRNAs are truly altered in promotion and initiation of RNA synthesis, rather than in transcription termination, RNA processing, or the stability of the result mRNAs.

We have already used the information obtained from this paper to aid us in the interpretation of data concerned with examining: (i) the viral and cellular components needed for promotion and initiation of SV40 RNA synthesis (25; J. E. Mertz, L. Trimble, T. J. Miller, and G. Z. Hertz, manuscript in preparation); and (ii) the reason for the transcriptional inactivity in vivo of linearized message-encoding templates (23). These experiments were feasible with the *Xenopus* oocyte system because we could: (i) perform short pulse-labeling experiments in vivo with radiolabeled triphosphates and thereby determine the rates of synthesis of viral RNA as well as steady-state levels; (ii) inject DNA molecules already in association with chromosomal proteins; (iii) follow the fate of the injected templates knowing that a majority of them were interacting with cellular components in a biologically meaningful manner; and (iv) recover both the injected samples and products made from them in quantities sufficient for a variety of biochemical analyses. Introduction of DNAs into mammalian fibroblasts by transfection or microinjection, although enabling one to use the natural host, lacks these other desirable features. In addition, although oocytes fail to regulate SV40 mRNA synthesis precisely in the manner observed in monkey cells, these quantitative differences may provide insights into the ways that different cell types may differentially affect regulation of expression of a mammalian operon.

MATERIALS AND METHODS

Microinjection of SV40 DNA and purification of RNA from oocytes. Early stage 6 oocytes, obtained as described previously (32), were injected intranuclearly with 10 nl of injection medium (24) containing 500 μg of supercoiled (form I) SV40 DNA per ml that had been purified from SV40-infected African green monkey kidney cells. Consequently, each oocyte received 5 ng of SV40 DNA or approximately 10^9 viral genomes. The techniques used for microinjection have also been described previously (32). After incubation at 19°C for approximately 24 h, the oocytes were labeled by microinjection into the animal pole of 20 nl of injection medium containing 25 mCi of [8-^{3}H]GTP (16 Ci/mmol) or [α-^{32}P]GTP (ca. 25 Ci/mmol) per ml. Oocytes were then placed in fresh HEPES (*N*-2-hydroxyethypiperazine-*N*′-2-ethanesulfonic acid)-modified Barth's solution (14). At appropriate times thereafter, the oocytes were harvested in groups of 10 to 20 by homogenization with an adjustable 1-ml pipettor in proteinase K buffer (50 μl per oocyte of 50 mM Tris-hydrochloride [pH 7.4], 10 mM EDTA, 1% sodium dodecyl sulfate [SDS], and 750 μg of proteinase K per ml). The homogenized oocytes were incubated at 37°C for 1 to 2 h, diluted with an equal volume of TES buffer (0.1 M Tris-hydrochloride [pH 9.0], 1 mM EDTA, 0.5% SDS), and extracted twice with phenol-chloroform-isoamyl alcohol (25:25:1). The organic phases were reextracted with TES. The nucleic acids in the resulting aqueous phases were combined and precipitated with ethanol. (Carrier was not added since *Xenopus* oocytes contain 4 μg of endogenous RNA.) After suspension in 0.25 ml of DNase I buffer (25 mM NaCl, 20 mM Tris-hydrochloride [pH 7.4], 5 mM $MgCl_2$, and 1 mM $CaCl_2$), each sample was incubated for 15 min at 37°C with 5 μl of DNase I (1 mg/ml in 1 mM HCl; Worthington, Biochemical Corp.), diluted to 1 ml in TES, extracted once with phenol-chloroform-isoamyl alcohol, precipitated with ethanol, and suspended in 0.1 × SSC (1× SSC is 0.15 M NaCl plus 0.015 M sodium citrate [pH 7.0])–0.2% SDS-0.2 mM EDTA at 5 μl per oocyte equivalent. Recoveries of acid-precipitable radiolabeled material were routinely greater than 95%.

Manual dissection of oocyte nuclei. Groups of 10 to 20 oocytes were pipetted into a 10-μl droplet of HEPES-modified Barth's solution placed on a piece of Parafilm stretched over the bottom of a 60-mm-diameter petri dish. Each oocyte was held stationary with a pair of watchmakers forceps while a microinjection needle (ca. 50-μm tip diameter) was used to poke a hole at the animal pole. The nucleus was extruded through the hole by gently squeezing the oocyte with the forceps, washed with HEPES-modified Barth's solution, and transferred to proteinase K buffer with a 50-μl pipette. Nuclei isolated in this manner were essentially free of cytoplasm. The droplet, containing the remainder of the oocyte and any material that leaked out of either the nuclei or cytoplasm of the oocytes during the nuclear isolation procedure, was transferred to a separate tube containing proteinase K buffer. Consequently, this latter material, although considered to be the

cytoplasmic fraction, was frequently contaminated with small amounts of nuclear RNA. Both the nuclear and cytoplasmic fractions were then homogenized separately, and the RNA was purified from them as described above.

Purification of poly(A)$^+$ RNA. Oligodeoxythymidylic acid cellulose (no. 7; Bethesda Research Laboratories, Inc.) was prepared and used to select for poly(A)$^+$ RNA essentially as described by Aviv and Leder (4).

Hybridization of SV40-specific RNA. One to six oocyte equivalents of purified RNA were incubated in 150 μl of 4× SSC–0.2% SDS at 67 to 68°C for 16 to 24 h in the presence of a 6.5-mm-diameter nitrocellulose filter (Millipore Corp.) containing ca. 0.125, 0.25, or 0.50 μg of denatured SV40 DNA fixed to the nitrocellulose as described by Raskas and Green (27). All samples were assayed in duplicate with filters containing different amounts of SV40 DNA to ensure that the hybridizations had been performed in DNA excess and that the values obtained were reproducible. Blank filters, prepared as described above but containing no SV40 DNA, were placed in the same hybridization reactions to determine the background levels of nonspecific binding of radioactivity to the filters. After incubation with RNA, each filter was washed extensively in 2× SSC at room temperature, treated with RNase A (10 to 50 μg/ml in 2× SSC) for 0.5 h at 37°C, washed again, and then dried. The amount of radioactivity that hybridized was determined by scintillation spectroscopy. Corrections were made for machine backgrounds of approximately 10 and 16 cpm for ^{3}H and ^{32}P, respectively.

The strand and region specificities of the radiolabeled SV40-specific RNAs were determined by hybridization of the purified RNAs to nitrocellulose strips containing an appropriate set of SV40 DNA restriction fragments. The RNAs were heated at 60°C for 1 to 2 min and then the hybridizations were performed at 68°C in 0.5 to 1.0 ml of 6× SSC–0.2% SDS–0.2 mM EDTA for 1 to 3 days. The filters were subsequently processed as described above, except that washes at 68°C in 2× SSC were also included. The pattern of bound radioactivity was determined by autoradiography.

The total amount of radioactivity incorporated into each RNA sample was determined by using DE81 filters. After application of the RNA, each filter was washed three times (5 min each) in 0.5 M sodium phosphate (Na_2HPO_4), twice in water, and twice in 95% ethanol. The amount of radioactivity that bound was determined by scintillation spectroscopy.

Formaldehyde-agarose gel electrophoresis. RNA samples to be sized by electrophoresis were precipitated with ethanol and suspended in 25 μl of running buffer (20 mM morpholine propanesulfonic acid [pH 7.0], 5 mM sodium acetate, 1 mM EDTA) containing 50% formamide–2.2 M formaldehyde. The samples were heated for 5 min at 60°C, made 10% sucrose and 0.2% bromophenol blue, applied to 1% agarose gels containing 2.2 M formaldehyde, and electrophoresed for 16 h at 50 V.

To determine which size classes of RNAs were SV40 specific, the RNAs were transferred out of the gel onto a nitrocellulose filter by using 20× SSC essentially as described by Southern (33) and Thomas (35). The filter was preincubated in 50% formamide–5× SSC–1× Denhardt buffer (0.2% bovine serum albumin, 0.2% Ficoll, 0.2% polyvinylpyrrolidone)–0.1% SDS and 10 μg of yeast RNA per ml for 5 h at 42°C and then hybridized with ^{32}P-labeled SV40 DNA for 16 h at 42°C in the same mixture lacking yeast RNA. Afterward, the filter was washed twice with 3× SSC–50% formamide for 15 min at 42°C; twice with 2× SSC–0.08% PP_i–0.1% SDS for 15 min at 42°C; six times in 1× SSC–0.08% PP_i–0.1% SDS for 30 min at 65°C; and then dried and autoradiographed.

Preparation of separated strands of the early and late regions of SV40 DNA. SV40 DNA was cleaved with the restriction endonucleases *Hpa*II and *Bam*HI, denatured with 0.15 N NaOH–0.02 M EDTA, and electrophoresed at 1 V/cm in a 1.5% agarose gel containing 36 mM Tris-hydrochloride–30 mM NaH_2PO_4–1 mM EDTA (pH 7.8) as the running buffer. The DNA was transferred from the gel onto nitrocellulose paper by using 20× SSC essentially as described by Southern (33).

Rate measurements and quantitation of data. The kinetics of accumulation and degradation of SV40 RNA were measured at various times after injection by hybridization of the ^{3}H-labeled oocyte RNA to SV40 DNA bound to filters. The efficiency of hybridization, measured by adding known amounts of in vitro synthesized ^{32}P-labeled SV40 RNA to the reaction, varied from 50 to 70%. Picomoles of GTP incorporated were converted to nanograms of RNA, assuming that the base composition (GMP) of SV40 RNA was 21% (36). The specific activity of the GTP pool for stage 6 oocytes is approximately 3,000 dpm/pmol based upon the similar labeling conditions employed by Anderson and Smith (3). Using the above information, we converted the amount of radioactivity bound to filters to picomoles and nanograms of newly synthesized SV40-specific RNA, assuming that 885 cpm = 1 pmol of GTP = 6 ng of SV40 RNA. Rate constants were calculated as described by Anderson and Smith (3). Rates of unstable RNA synthesis were determined from the equation $dC/dt = K_{us} - K_dC$, where C is the amount of radiolabeled unstable RNA, K_{us} is the rate of synthesis of unstable RNA in units of mass per unit of time, and K_d is the decay constant, which is considered to be first order and is in units of reciprocal time (K_d = In 2 divided by the half-life). K_s, the synthetic rate constant of stable RNA accumulation, equals dC_s/dt, where C_s is the amount of stable radiolabeled RNA.

Measurement of the rate of degradation of SV40 RNA was performed by injecting radiolabeled oocytes intranuclearly with 10 nl of α-amanitin (100 μg/ml). Assuming that the α-amanitin disperses throughout the oocyte and that an oocyte is approximately 1 μl in volume, this gives a final α-amanitin concentration of 1 μg/ml. This concentration inhibits greater than 95% of RNA polymerase II activity (15, 30; T. J. Miller and J. E. Mertz, unpublished data) and therefore serves as an effective chase for radiolabeled SV40 RNA. The decay constants were estimated at appropriate times from the slopes of the lines indicating radioactive SV40 RNA versus time after addition of α-amanitin as plotted on semi-logarithmic paper.

RESULTS

RNA synthesis and degradation in full-grown oocytes. The kinetics of accumulation of SV40

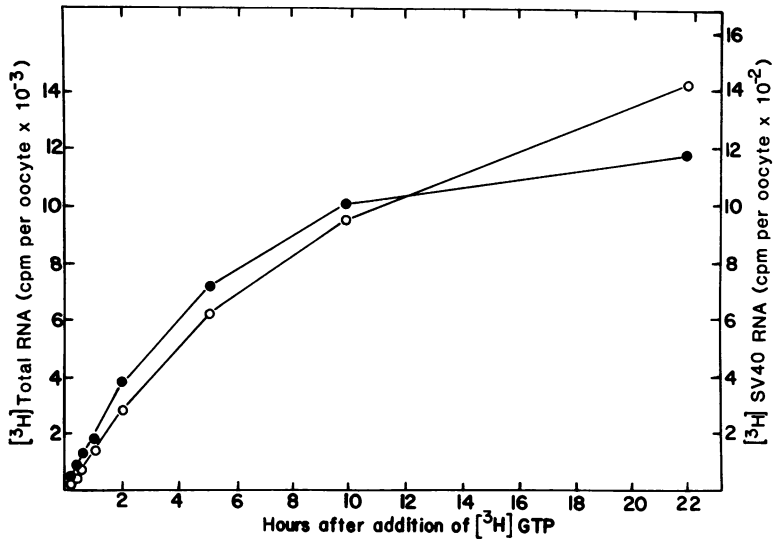

FIG. 1. Synthesis of total RNA (O) versus SV40 RNA (●) in *Xenopus* oocytes. Groups of 30 oocytes were microinjected with 10 nl of a 500-μg/ml solution of SV40 DNA. Twenty-four hours later, [^{3}H] GTP (20 nl of a 25-mCi/ml solution at 16 Ci/mmol) was added. At various times thereafter, oocytes were harvested and their RNA purified as described in the text. Total radiolabeled RNA was determined with a DE81 filter binding assay (see the text) which retains all RNA larger than 5 to 8 nucleotides in size. ^{3}H-labeled SV40-specific RNA was determined by hybridization to SV40 DNA bound to filters.

and total oocyte RNA in early stage 6 oocytes are shown in Fig. 1, and the kinetics of degradation of SV40 RNA is presented in Fig. 2. Since the latter curve is clearly biphasic, we analyzed both sets of data assuming that the RNAs contain short-lived and long-lived components. In addition, Anderson and Smith (3) have shown that the pool of GTP decreases less than 10% during a 24-h incubation period under experimental conditions similar to those employed by us. Consequently, the decreases with time in the rates of accumulation of the radiolabeled RNAs

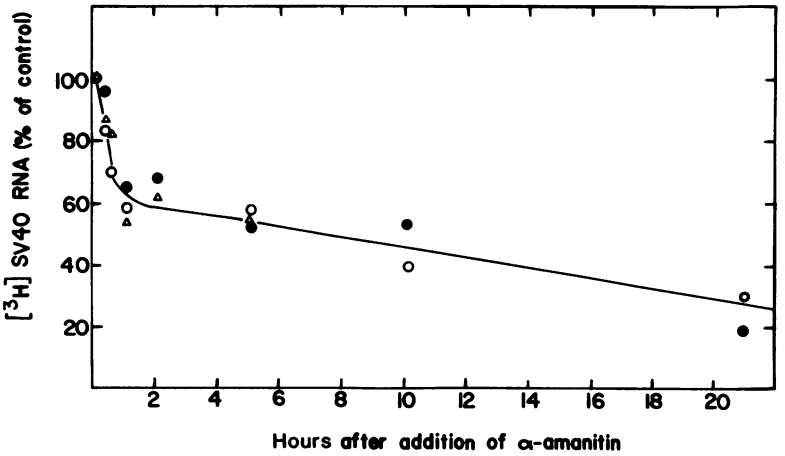

FIG. 2. Disappearance of radiolabeled SV40-specific RNA under chase conditions. Groups of 30 oocytes were microinjected intranuclearly with 20 nl of injection buffer containing 250 μg of SV40 DNA and 25 mCi of [^{3}H]GTP (16 Ci/mmol) per ml. Twenty-four hours later, 10 nl of α-amanitin (100 μg/ml) was injected and the incubation continued until being terminated at the indicated times. The RNA from each group of oocytes was purified and analyzed for SV40-specific RNA as described in the text. The data points, taken from three separate experiments, were normalized to the amount of radioactivity present per oocyte at the time of addition of α-amanitin.

(Fig. 1) were unlikely to be due to changes in either the concentrations or the specific activities of the radiolabeled GTP. Therefore, we calculated approximate rate constants for the various components of RNA as described above by using the assumption that the pool of radiolabeled GTP remains constant throughout the course of each experiment.

Table 1 gives a summary of the rate constants and half-lives calculated from the data in Fig. 1 for the unstable (K_{us}) and stable (K_s) components of total endogenous and SV40-specific RNA synthesized in oocytes injected intranuclearly with 5 ng (ca. 10^9 molecules) of SV40 DNA. The results agree well with those reported previously by Anderson and Smith (3) and show that: (i) the half-lives of the unstable components of these RNAs were ca. 15 to 30 min; (ii) the initial rate of accumulation of SV40 RNA under these experimental conditions was approximately one-tenth of that for total oocyte RNA; and (iii) approximately one quarter of the total endogenous RNA synthesized was long-lived.

Independent estimates of the half-lives of the unstable and stable species of SV40 RNA were obtained from data on the kinetics of degradation of radiolabeled SV40 RNA (Fig. 2). In this experiment, the oocytes were preincubated for 24 h with SV40 DNA and [^{3}H]GTP to label maximally both the stable and unstable species of viral RNA. The oocytes were then injected with α-amanitin (final concentration, 1 μg/ml) to inhibit further synthesis of SV40-specific RNA. From these latter data, the half-lives of the unstable and stable components of SV40 RNA were estimated to be approximately 37 min and 17 h, respectively.

Cellular distribution of newly synthesized RNA. To determine the partitioning between the nucleus and cytoplasm of the unstable and stable components of newly synthesized RNA, a time course experiment similar to the one described in Fig. 1 was performed, except the oocytes were fractionated into nuclear and cytoplasmic components. The data in Fig. 3A and B indicate that the amounts of both total nuclear and SV40 RNA reached steady-state values within approximately 5 h after the addition of [^{3}H]GTP. Therefore, much of the newly synthesized RNA was unstable, a finding consistent with fairly rapid turnover of most of the RNA in the nucleus combined with transport of some of the RNA to the cytoplasm. The rate constants and half-lives calculated from these data are summarized in Table 1. From these numbers we conclude that the vast majority of the RNA synthesized in the nucleus of oocytes was either degraded or transported to the cytoplasm where it accumulated at approximately 0.4 pmol per oocyte per h. Likewise, the numbers obtained for the SV40-specific RNA were qualitatively similar, but an order of magnitude lower; essentially all of the SV40 RNA was either degraded or transported to the cytoplasm where it accumulated at approximately 0.017 pmol of GTP or 0.1 ng of RNA per oocyte per h (Table 1).

Rates of accumulation of poly(A)$^+$ SV40 RNA.

TABLE 1. Summary of endogenous and SV40-specific RNA synthesis in stage 6 oocytes

RNA type	Synthesis parameter[a]			
	K_{us} (pmol GTP incorporated/h per oocyte)	K_s (pmol GTP incorporated/h per oocyte)	Half-life of unstable component (min)	Rate of cytoplasmic RNA accumulation (pmol GTP incorporated/h per oocyte)
Oocyte RNA				
Total RNA	1.6 (1.6)	0.5 (0.5)	18 (21)	0.4
Total nuclear RNA	1.4	0.09	14	
Total poly(A)$^+$ RNA	0.03	0.02	20	0.02
SV40-specific RNA				
Total SV40	0.18 (0.18)	0.02 (0.02)	19 (24)	0.017
Total nuclear SV40 RNA	0.16	0.002	15	
Total poly(A)$^+$ SV40 RNA	0.014	0.003	21	0.002
Nuclear poly(A)$^+$ SV40 RNA	0.011	~0.001	18	
Total poly(A)$^-$ SV40 RNA	0.16	0.02	25	0.016
Nuclear poly(A)$^-$ SV40 RNA	0.10	0.01	22	

[a] The numbers in parentheses were calculated as described in the text from the data presented in Fig. 1; all of the others were obtained from the experiments in Fig. 3 and 4. Variations of as much as a few fold may exist from one batch of oocytes to the next.

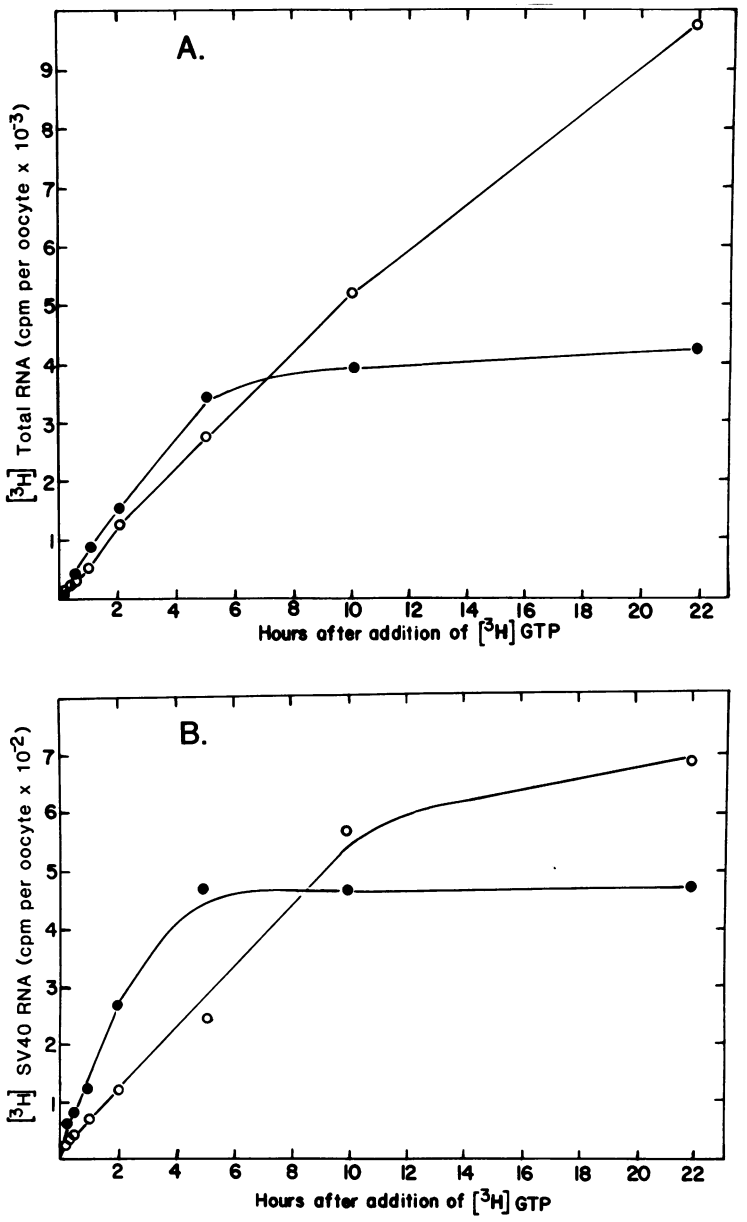

FIG. 3. Kinetics of accumulation of (A) endogenous and (B) SV40-specific RNA in the nuclei (●) and cytoplasm (○) of oocytes. SV40 DNA (5 ng per oocyte) was injected intranuclearly into oocytes. Twenty-four hours later [^{3}H]GTP (20 nl per oocyte; 25 mCi/ml, 16 Ci/mmol) was added. At various times thereafter, the nuclei were manually dissected out of groups of oocytes as described in the text. Immediately afterwards, the RNA samples from the nuclear and cytoplasmic fractions were incubated with proteinase K buffer. Subsequently, they were purified and analyzed for both total and SV40-specific radiolabeled RNA as described in the text.

The rates of accumulation of poly(A)$^+$ and poly(A)$^-$ SV40 RNA in the nucleus and cytoplasm were determined by fractionation of the purified nuclear and cytoplasmic components of RNA on oligodeoxythymidylic acid-cellulose columns. The data are shown in Fig. 4A and B. Tables 1 and 2 summarize the results. The data for the nuclear RNAs were qualitatively similar to those already discussed above. Two findings are noteworthy: (i) one-third to one-half of the poly(A)$^+$ RNA initially made in these oocytes was SV40 specific, a result indicating that much of the mRNA synthesis occurring in the SV40 DNA-injected oocytes was directed by the in-

jected template; and (ii) most of the newly synthesized virus-specific RNA was not polyadenylated.

The data on the kinetics of appearance in the cytoplasm of the poly(A)$^+$ and poly(A)$^-$ SV40 RNAs are also indicated in Fig. 4A and B, respectively, and in Tables 1 and 2. As with total oocyte poly(A)$^+$ cytoplasmic RNA (data not shown), the poly(A)$^+$ SV40 RNA exhibited an initial lag period of approximately 1 h; afterward, it accumulated in the cytoplasm at a rate of approximately 11 pg of RNA per oocyte per hour or approximately 9% of the rate seen for poly(A)$^+$ total oocyte RNA (data not shown). These lags corresponded well with the length of time it took the nuclear poly(A)$^+$ RNA to reach a steady-state value. This finding indicates, as expected, that the stable cytoplasmic poly(A)$^+$ RNA resulted from processing and transport of some of the "unstable" nuclear RNA. The fact that the poly(A)$^+$ SV40 RNA represented less than 1% of the total radiolabeled oocyte RNA in the cytoplasm was probably due to most of the newly synthesized stable oocyte RNA being 18S and 28S rRNA.

On the other hand, the amount of radiolabeled poly(A)$^-$ SV40-specific RNA reached a plateau value within 10 h. This latter finding indicates that a steady-state was reached in which the poly (A)$^-$ virus-specific cytoplasmic RNA was degraded as rapidly as newly synthesized SV40 RNA was transported there from the nucleus. It is also noteworthy that most of the virus-specific RNA accumulating in the cytoplasm at early times was not polyadenylated (Table 1).

Some of the poly(A)$^-$ RNA seen in these experiments may have resulted from cleavage of poly(A)$^+$ RNA by nonspecific nucleases. However, since the kinetics of accumulation of these two classes of RNAs were quite different, such an experimental artifact could account for only a small percentage of the poly(A)$^-$ RNA.

Sizes of the short-lived and steady-state species of virus-specific RNAs synthesized in SV40 DNA-injected oocytes. The finding that less than 10% of the SV40-specific RNA was long-lived indicates either that a fairly large percentage of the primary transcripts were degraded complete or that they were processed to stable RNAs that were, on average, severalfold smaller in size. To distinguish between these two possibilities, we examined by electrophoresis in denaturing formaldehyde-agarose gels the sizes of the short-lived and steady-state species of SV40 RNAs made in SV40 DNA-injected oocytes. To determine the sizes of the short-lived species, we radiolabeled SV40 DNA-injected oocytes during the last 4 h of a 28-h incubation period. Lanes A and B of Fig. 6 show the newly synthesized RNAs produced by uninjected and SV40 DNA-injected oocytes, respectively. The most apparent difference between them is the existence in lane B of a heterogeneous collection of RNAs ranging in size from slightly greater than 40S rRNA up to ones too large to enter the gel. Presumably, these large RNAs are primary transcripts that result from RNA polymerase II transcribing SV40 DNA several complete turns around the circular template before terminating. Multigenomic length transcripts of this type are known to exist in SV40- and polyoma virus-infected mammalian cells (see ref. 36 for a review of this topic).

The sizes of the steady-state species of SV40-specific RNAs were determined by Northern blot analysis by using the nonradiolabeled RNA present in oocytes that had been allowed to synthesize, process, and accumulate SV40 RNA for 2 days. As with the size data obtained previously with sucrose gradients (20, 30), three

TABLE 2. Time course and distribution of newly synthesized SV40-specific RNA species between the nucleus and cytoplasm of oocytes[a]

Time after addition of [^{3}H]GTP	% Total oocyte RNA		% Poly(A)$^+$ SV40 RNA		% Radiolabeled poly(A)$^+$ nuclear RNA which was SV40 specific	% Radiolabeled poly(A)$^+$ cytoplasmic RNA which was SV40 specific	SV40 poly(A)$^+$ RNA as % total oocyte RNA
	Nucleus	Cytoplasm	Nucleus	Cytoplasm			
20 min	55	45	61	39	71	27	1.4
30 min	60	40	75	25	53	40	1.5
1 h	55	45	72	28	46	18	1.1
2 h	63	37	54	46	48	15	1.0
5 h	57	43	33	67	28	17	0.4
10 h	43	57	24	76	31	19	0.5
22 h	29	71	13	87	32	11	0.6

[a] These values were derived from the experiment described in Fig. 4; variations of as much as a few fold may exist from one batch of oocytes to the next.

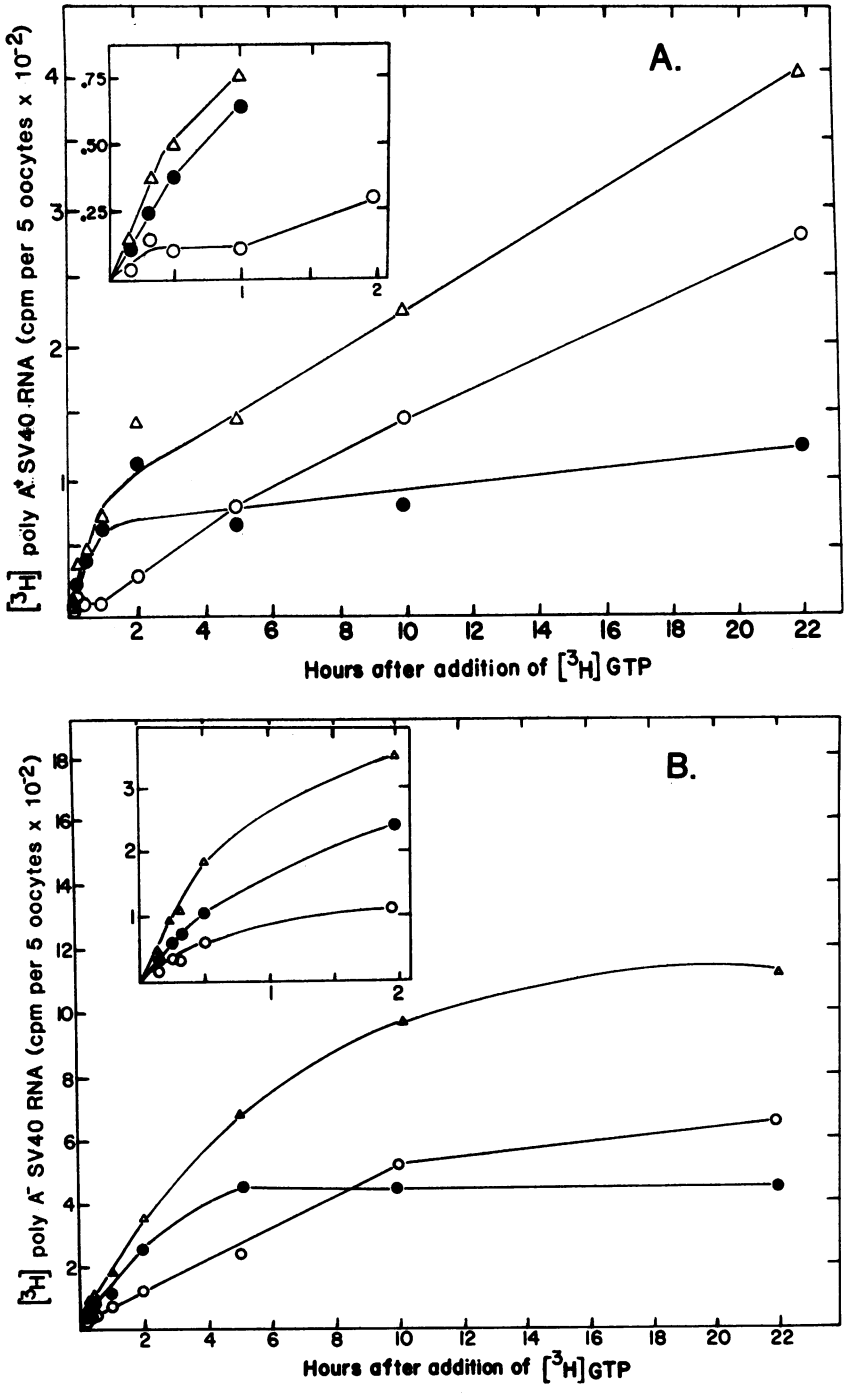

FIG. 4. Kinetics of accumulation of (A) poly(A)$^+$ and (B) poly(A)$^-$ SV40-specific RNA in the nucleus and cytoplasm of oocytes. SV40 DNA and, subsequently, [^{3}H]GTP were injected into oocytes as described in the legend to Fig. 3. At various times thereafter, the nuclear and cytoplasmic portions of groups of oocytes were manually separated. Each RNA sample was purified separately, followed by fractionation with oligodeoxythymidylate cellulose chromatography as described in the text. The inserts show magnified versions of the data from the earliest time points. Symbols: ●, nuclear RNA; ○, cytoplasmic RNA; △, sum of nuclear plus cytoplasmic RNA.

regions of the resulting autoradiogram (not shown) were noteworthy: (i) a diffuse band that probably corresponds to the heterogeneous mixture of stable late 19S RNAs seen in SV40-infected monkey cells (see Fig. 5 and data presented below); (ii) a smear of large RNA ranging in size from approximately 28S up to much greater than 40S; and (iii) a diffuse band of RNA approximately 4S in size. Since this 4S RNA was detectable by using the *Hin*dIII-C restriction fragment of SV40 (see Fig. 5) as the radiolabeled probe, it must include at least part of the 0.65 to 0.86 region of the SV40 genome. Quite likely, this 4S RNA corresponds to the small viral RNA seen in SV40-infected monkey cells that is presumed to result from transcriptional attenuation (18).

Precise structural analysis of the viral RNAs made from wild-type SV40 DNA is rather difficult to do because the RNAs are large in size and very heterogeneous with respect to both their 5′ ends and spliced out regions (see ref. 36 for review). To simplify our problem somewhat, we also performed these experiments with the *Hin*dIII-C restriction fragment of SV40 (map position 0.65 to 0.86; see Fig. 5). This fragment of SV40 DNA contains all of the regulatory sequences involved in promotion and initiation of viral RNA synthesis and is as transcriptionally active as wild-type SV40 DNA when injected into oocytes in a ligated circular form (25; Mertz et al., in preparation). Lanes C and D of Fig. 6 show the newly synthesized RNAs produced in oocytes radiolabeled from 24 to 28 h after the injection of this DNA fragment in the absence or presence of α-amanitin, respectively. As with wild-type SV40 DNA, large (>40S) RNAs, whose synthesis was prevented by α-amanitin, were produced in large quantity. Presumably, these RNAs resulted from RNA polymerase II circumscribing this tiny (1,118 nucleotide pair) DNA template over and over again in the absence of transcription termination or rapid processing of the primary transcript. Several distinct bands, indicative of site-specific RNA processing, were also apparent.

The Northern blot analyses presented in lanes F and G of Fig. 6 confirm that these smaller bands of RNA are SV40 specific. Most of the steady-state viral RNA produced in oocytes injected with the *Hin*dIII-C DNA migrated as a single species approximately 14S in size. This species of RNA was also present, but only as a minor component, in the 4-h labeling experiment (lane C). A band of somewhat larger RNA, migrating at approximately 21S, is also visible in both lanes C and G. These two RNA species may be transcripts with sizes approximately the same and twice the length of the *Hin*dIII-C fragment. The existence of a series of RNA species of approximately integral multiples of the template in size, together with the data on the kinetics of their synthesis, indicates a possible precursor-product relationship between the larger and smaller RNAs, with the 14S species being the ultimate final stable product.

Strand and sequence specificities of the viral RNAs synthesized in oocytes. If the large initial transcripts that contain sequences from the entire genome are processed properly in oocytes to yield stable mRNAs and nonmessage byproducts that get degraded fairly rapidly, the SV40-specific RNAs present at steady state should hybridize preferentially with the message-encoding sequences of the viral genome. To determine whether this is the case, we labeled oocytes with [^{32}P]GTP from 24 to 48 h after injection with wild-type SV40 DNA or the *Hin*dIII-C restriction fragment. The radiolabeled RNA was purified and hybridized to nitrocellulose strips containing separated strands of the early and late regions of the SV40 genome (Fig. 7).

The data resulting from this experiment (Fig. 7, lane 2) indicate that approximately two-thirds of the steady-state RNA made in wild-type SV40

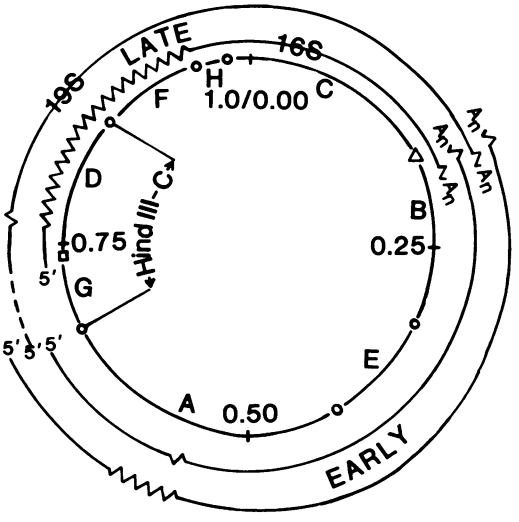

FIG. 5. Map of the SV40 genome. The restriction fragments generated by cleavage of SV40 DNA with the restriction endonucleases *Hin*dIII (○), *Bam*HI (△), and *Hpa*II (□) are indicated. The curved lines indicate the structures of the viral mRNA species seen in monkey cells at early and late times after infection with SV40. The wavy area of each line shows the region of the initial transcript that gets spliced out during synthesis of the mRNA. The broken region of the late 19S mRNA indicates that this mRNA species exhibits heterogeneity at its 5′ end. Not shown here is the fact that the 19S mRNAs are also heterogeneous with respect to the 3′ ends of their leader segments (36).

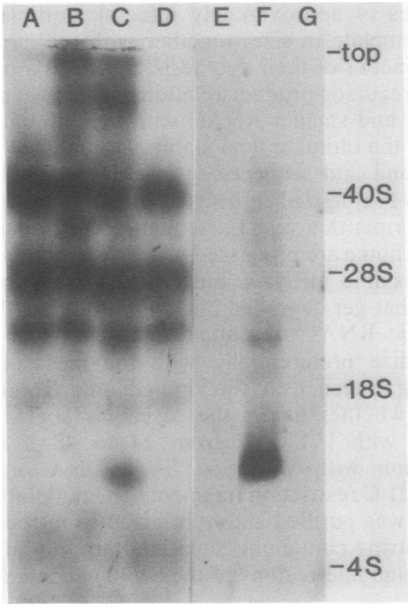

FIG. 6. Sizes of the stable and short-lived species of RNAs made in oocytes injected with wild-type SV40 DNA (lane B) and circularized purified *Hin*dIII-C restriction fragment of SV40 DNA (lanes C and F). Oocytes were injected intranuclearly with 10 nl of wild-type SV40 form I DNA (500 μg/ml) or cloned, agarose gel-purified *Hin*dIII-C fragment of SV40 DNA (150 μg/ml) that had been circularized before injection by treatment with T4 DNA ligase at low DNA concentration to prevent oligomer formation. For lanes A through D, the oocytes were injected with [α^{32}P]GTP 24 h after the DNA samples had been added. All oocytes were harvested at 28 h after injection of the DNA samples by homogenization in proteinase K buffer. After purification, the RNAs in each sample were sized by electrophoresis in a formaldehyde-agarose gel (see text for details). The oocyte RNAs shown in lanes A through D, having been pulse-labeled in vivo, were visualized directly by autoradiography. Those in lanes E through G were analyzed for SV40-specific sequences by transfer to nitrocellulose paper, hybridization with the *Hin*dIII-C restriction fragment of SV40 DNA ^{32}P-labeled in vitro by nick-translation (28), and autoradiography (see text for details). The size markers, visualized by UV fluorescence of ethidium bromide-stained RNA, were brome mosaic virus RNAs (903, 2,419, 3,193, and 3,516 nucleotides in length), the oocyte 40S, 28S, and 18S rRNAs, and yeast 4S transfer RNA. A and E, RNA from oocytes not injected with SV40 DNA as a control; B, RNA from oocytes injected with wild-type SV40 DNA; C and F, RNA from oocytes injected with the *Hin*dIII-C fragment of SV40; and D and G, same as C and F with α-amanitin (100 μg/ml) coinjected with the DNA.

DNA-injected oocytes was synthesized from the late region of the late strand. This is the region from which late 19S mRNA from infected monkey cells is also made (see Fig. 5). Most of the remainder hybridized to the early region of the late strand. This result is consistent with our finding that viral RNAs greater than the entire genome in length were also present (Fig. 6). Taken together, these data indicate that most of the SV40 RNA made in oocytes was transcribed from the late strand and that the initial transcripts corresponded to one or more complete times around the SV40 genome. In addition, they are consistent with the hypothesis that these large RNAs were gradually processed to the stable late-strand mRNAs seen in SV40-infected monkey cells, with concomitant degradation of the nonmessenger byproducts.

Approximately 4% of the SV40 RNA hybridized to the early region of the early strand. However, because of the presence of larger

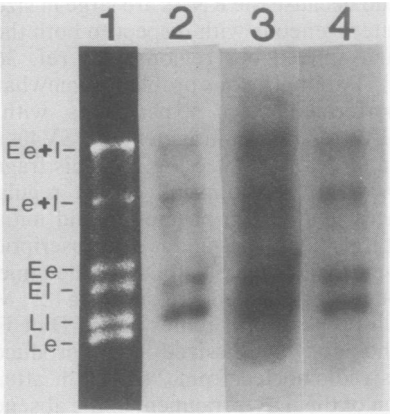

FIG. 7. Strand specificity of the SV40 RNA made from SV40 DNA-injected oocytes. Oocytes were injected intranuclearly with wild-type SV40 form I or circularized purified SV40 *Hin*dIII-C DNA as described in the legend to Fig. 6. [α-^{32}P]GTP was injected 24 h later, and incubation was continued for an additional 24 h. The resulting radiolabeled RNAs were purified and hybridized to nitrocellulose strips containing separated strands of the *Hpa*II-*Bam*HI restriction fragment pattern of SV40 DNA (see text for details). E and L indicate the early and late regions, respectively, of the SV40 genome separated roughly by the *Hpa*II and *Bam*HI restriction endonuclease cleavage sites (see Fig. 5). e and l indicate, respectively, the strands of the viral genome from which early and late SV40 mRNAs are made in monkey cells. Lane 1, pattern of strand-separated restriction fragments in the agarose gel as visualized by UV fluorescence of ethidium bromide-stained DNA before transfer to nitrocellulose paper; lane 2, autoradiograph of a nitrocellulose strip incubated with the ^{32}P-labeled RNA made in oocytes injected with wild-type SV40 form I DNA; lane 3, same as lane 2, but exposed twice as long; and lane 4, autoradiograph of a nitrocellulose strip incubated with the ^{32}P-labeled RNA made in oocytes injected with circularized purified SV40 *Hin*dIII-C DNA.

amounts of complementary RNA synthesized from the early region of the late strand, this number is probably an underestimate. Nevertheless, we can conclude from this experiment that the relative accumulation of early- versus late-strand RNA present in oocytes corresponds with what is seen late, rather than early, in infection of monkey cells.

The data obtained from the *Hin*dIII-C DNA-injected oocytes (Fig. 7, lane 4) confirms the above findings. Once again, most of the viral RNA hybridized with the late region of the late strand, some early region-late strand RNA was observed, and little, if any, stable early-strand RNA was present.

DISCUSSION

The data presented here on the rates of accumulation of SV40 and endogenous RNA agree well with those reported by Anderson and Smith (3). We found that SV40 DNA microinjected into the nucleus of *Xenopus laevis* stage 6 oocytes is transcribed by RNA polymerase II and exhibits many of the characteristics of heterogeneous nuclear RNA synthesis including: (i) primary transcripts much larger than the mRNAs in size; (ii) biphasic kinetics with a large portion of the RNA turning over in the nucleus with a short half-life; (iii) polyadenylation and processing of the RNA; and (iv) a relatively slow, constant rate of accumulation of the RNA in the cytoplasm after a short lag.

A comparison of the rates of accumulation in the cytoplasm of SV40 versus endogenous poly(A)$^+$ RNA indicates that SV40 RNA represents only 10% of the total. However, the rate of accumulation of endogenous cytoplasmic poly(A)$^+$ RNA includes that occurring in the mitochondria. Therefore, much of the transcription involving RNA polymerase II is directed by the injected template. Given a constant rate of accumulation of 11 pg per oocyte per h, approximately 0.2 ng of poly(A)$^+$ SV40 RNA would be present in the cytoplasm after 1 day. Previous work on endogenous poly(A)$^+$ RNA in stage 6 oocytes showed that only 10% of it is bound to polysomes (11, 29). Consequently, the observation that injected DNAs are actively transcribed but translated at rather low levels (9, 26) may be due to a combination of: (i) only a small percentage of the newly synthesized RNA becoming stable poly(A)$^+$ cytoplasmic RNA; and (ii) only a fraction of this latter RNA becoming polysomal.

One peculiar observation was the finding that most of the SV40 RNA synthesized remained poly(A)$^-$, or at most contained a stretch of poly(A) too short to allow binding to oligodeoxythymidylic acid. Some of this poly(A)$^-$ RNA was transported to the cytoplasm. However, unlike the poly(A)$^+$ SV40 RNA, it was not stable (Fig. 4B). The reason for this phenomenon is unclear, but may indicate that transport of RNA to the cytoplasm can precede polyadenylation.

Synthesis and processing of SV40 RNA in *Xenopus* oocytes is similar to that seen late in infection of mammalian cells by papova viruses. The data presented here on the kinetics of synthesis and processing of viral RNA in SV40 DNA-injected stage 6 oocytes of *Xenopus laevis* are very similar to those observed for polyoma virus-infected mouse cells (see ref. 36 for review of the polyoma virus literature). Acheson (1) has proposed that the poor efficiency of processing of late viral RNA in mouse cells is due to: (i) the presence in nuclear transcripts of non-mRNA sequences that are removed during processing; (ii) the presence in nuclear transcripts of multiple copies of mRNA sequences, only one of which is incorporated into mature mRNA; (iii) inefficient polyadenylation of viral nuclear RNA; and (iv) some transcripts being completely degraded after incorrect processing.

The kinetics of synthesis of viral RNA in SV40-infected monkey cells has been reported by Aloni et al. (2) and Chiu et al. (7). As with polyoma virus, the nuclear viral RNA also decays in a multiphasic manner, with much of the RNA turning over rapidly in the nucleus. However, SV40 RNA synthesis in monkey cells differs from polyoma virus RNA synthesis in that: (i) although late strand transcription does proceed beyond the site of polyadenylation (13), giant nuclear transcripts are present, but as a very minor species in SV40-infected monkey cells; (ii) the unstable nuclear component is degraded with a half-life of only 8 min; and (iii) 30 to 40% of the viral RNA is transported to the cytoplasm. All of these differences in the kinetics of synthesis and processing of the RNAs of these two closely related viruses disappear if one hypothesizes that RNA processing proceeds more rapidly in monkey cells than in mouse cells. In addition, Anderson and Smith (3) have shown that processing and transport of RNA occur slowly in stage 6 oocytes. We therefore conclude that SV40 DNA is being transcribed faithfully in oocytes and that the differences seen in the kinetics of synthesis and processing of SV40 RNA in *Xenopus* oocytes versus monkey cells are probably due solely to quantitative differences in the rates at which these cells process newly synthesized RNAs.

One puzzling finding was the observation that most of the viral RNA was synthesized from the late strand (Fig. 7). When papova viruses first infect mammalian cells, a majority of the newly synthesized viral RNA is transcribed from the early strand. Only after the virus-encoded tumor

antigens are produced and the viral DNA begins to replicate does transcription switch to being mostly from the late strand (see ref. 36 for review). However, SV40 DNA does not replicate in stage 6 oocytes of *Xenopus laevis* (17). Furthermore, the *Hin*dIII-C fragment of SV40, which lacks the region of the genome that encodes the tumor antigens, also synthesized mostly late-strand transcripts in oocytes (Fig. 7, lane 4). Consequently, neither viral DNA replication nor the virus-encoded tumor antigens appear to be essential for late-strand RNA synthesis in oocytes. One possible explanation for this unexpected finding is that oocytes, being germ line cells, may already contain one or more proteins equivalent to the tumor antigens that papova viruses introduce into differentiated cells. Consistent with this idea is the existence of cellular proteins that react with antibodies directed against SV40 T-antigen (8, 34). Alternatively, the switch to predominantly late-strand RNA synthesis may result from a large number or concentration of viral templates being present. Considering that the concentration of viral DNA molecules we placed in each oocyte was equivalent to approximately 10^4 molecules per monkey cell, we may have simply bypassed the early stages of the viral lytic cycle.

Oocytes as a system for studying various regulatory and mechanistic aspects of mRNA biogenesis. Specific size classes of RNAs are produced from circular DNA templates injected into oocytes (Fig. 6) (20, 30; M. Wickens, personal communication). Therefore, at least some of the initial transcripts are processed to molecules with similar 5′ and 3′ termini. The data presented in Fig. 4A show that poly $(A)^+$ SV40-specific RNA accumulates in oocytes. M. Wickens (personal communication) has demonstrated by S1 mapping that at least some of the viral RNA made in SV40 DNA-injected oocytes has its 3′ end located at the polyadenylation site used in monkey cells. We, therefore, conclude that oocytes can process initial transcripts to produce correctly polyadenylated 3′ termini.

The existence of transcripts greater than one genome length in size confirms the data of Ford and Hsu (13), which demonstrate that transcription can proceed beyond the polyadenylation site. Fitzgerald and Shenk (12) have also observed this phenomenon with a mutant of SV40 that contains a tandem duplication of a region of the viral genome including the polyadenylation site at map position 0.17. How the cellular processing enzymes determine which of two or more identical polyadenylation sites to use is not yet known. The data presented here indicate that both transcriptional termination and polyadenylation occur very slowly in stage 6 oocytes and that polyadenylation may occur at the second, third, or even fourth, rather than first copy of the wild-type SV40 polyadenylation sites present in large multigenomic length initial transcripts.

The injection of the *Hin*dIII-C restriction fragment (0.65 to 0.86 map units) of SV40 DNA also resulted in the synthesis of specific size classes of RNAs (Fig. 6, lane F), in spite of the absence of a known polyadenylation site. Lebowitz and Weissman (21) have noted that a bacteria-like potential transcription termination signal exists at map position 0.74. Hay et al. (18) have observed termination at this site in vitro with transcription complexes isolated from SV40-infected monkey cells. Since most of the steady-state viral RNA made from the *Hin*dIII-C fragment was approximately unit-length (14S or ca. 1,000 to 1,200 nucleotides) and specific for the late strand (Fig. 7, lane D), we propose that, as with wild-type SV40 infection of monkey cells, its 5′ end is located at map position 0.67 to 0.72, but its 3′ end is located at this transcriptional attenuator site. If termination were less than 100% efficient, it would result in the production of the 4S RNA, approximately genomic length RNA, twice unit-length RNA, etc., that were seen. Consistent with this hypothesis is our finding that the SV40-specific RNA made in *Hin*dIII-C fragment DNA-injected oocytes is not polyadenylated (data not shown).

The 5′ ends of the stable mRNAs that are produced in SV40-infected monkey cells are very heterogeneous in sequence, spanning the 0.67 to 0.72 region of the viral genome (see ref. 36 for review). Consequently, we have not yet attempted to determine precisely the map positions of the 5′ ends of the viral RNAs made in oocytes. Nevertheless, we believe that they are probably similar to those seen in monkey cells based upon promoter mapping data (Mertz et al., in preparation) that show that the same sequences on the viral genome are essential for SV40 RNA synthesis in both oocytes and monkey cells.

The biogenesis of SV40 mRNAs also involves the excision of intervening sequences present in the initial transcripts (see ref. 36 for review). Our laboratory (G. Z. Hertz and J. E. Mertz, unpublished data) and others (M. Wickens, personal communication) have examined, by S1 mapping (5) with a 5′ end-labeled DNA probe, the structure of the late-strand viral RNAs made when SV40 DNA is injected into oocytes. Preliminary results show that the acceptor site usually used for splicing in oocytes is probably identical to that used in the production of the late 19S, rather than the 16S, viral mRNA that normally predominates in SV40-infected monkey cells. The locations of the donor sites used for splicing have not yet been determined be-

cause several may be employed. In addition, since the primary transcripts are multigenomic in length, the leader regions of the processed stable RNAs are likely to contain small tandem repeats that are generated when slightly less than genomic length segments of RNA are excised. Therefore, nucleotide sequence analysis of individual RNA species will be needed to determine definitively the structures of the 5′ ends of the viral RNAs made in oocytes. In the absence of such data, we rely on coupled transcription-translation experiments (9, 13a, 31, 37) to conclude that oocytes can correctly process at least some of the RNA molecules they synthesize from injected DNA templates.

In summary, differences were noted in strand preference, efficiencies of transcription termination and polyadenylation, and the splice sites used in the synthesis and processing of SV40 RNA in *Xenopus* oocytes and monkey cells. However, since these differences were quantitative rather than qualitative in nature, they were probably due to regulatory, rather than mechanistic, differences between the two cell types. We therefore conclude that *Xenopus* oocytes may be a useful system for studying various mechanistic aspects of mRNA biogenesis including: DNA template requirements for initiation of RNA synthesis, polyadenylation, and RNA splicing; precursor-product relationships among related RNA species; the order of RNA processing events; and the partitioning between the nucleus and cytoplasm of intermediates in RNA processing. In addition, although oocytes fail to regulate SV40 mRNA synthesis precisely in the manner observed in monkey cells, these quantitative differences may provide insights into the ways that different cell types may differentially affect regulation of expression of a mammalian operon.

ACKNOWLEDGMENTS

We wish to thank Jeff Ross, L. Dennis Smith, Bill Sugden, and Howard Temin for helpful comments on the manuscript and Catharine Conley for artistic assistance.

This work was supported by Public Health Service grants CA-07175 and CA-22443 from the National Cancer Institute. T.J.M. was supported by Public Health Service training grant CA-07075 and fellowship PF-1678 from the American Cancer Society.

LITERATURE CITED

1. **Acheson, N. H.** 1981. Efficiency of processing of viral RNA during the early and late phases of productive infection by polyoma virus. J. Virol. **37**:628–635.
2. **Aloni, Y., M. Shani, and Y. Reuveni.** 1975. RNAs of simian virus 40 in productively infected monkey cells: kinetics of formation and decay in enucleate cells. Proc. Natl. Acad. Sci. U.S.A. **72**:2587–2591.
3. **Anderson, D. M., and L. D. Smith.** 1977. Synthesis of heterogenous nuclear RNA in full-grown oocytes of *Xenopus laevis* (Daudin). Cell **11**:663–671.
4. **Aviv, H., and P. Leder.** 1972. Purification of biologically active globin messenger RNA by chromatography on oligothymidylic acid-cellulose. Proc. Natl. Acad. Sci U.S.A. **69**:1408–1412.
5. **Berk, A. J., and P. A. Sharp.** 1977. Sizing and mapping of early adenovirus mRNAs by gel electrophoresis of S1 endonuclease-digested hybrids. Cell **12**:721–732.
6. **Brown, D. D., and J. B. Gurdon.** 1977. High-fidelity transcription of 5S DNA injected into *Xenopus* oocytes. Proc. Natl. Acad. Sci. U.S.A. **74**:2064–2068.
7. **Chiu, N. H., M. F. Radonovich, M. M. Thoren, and N. P. Salzman.** 1978. Selective degradation of newly synthesized nonmessenger simian virus 40 transcripts. J. Virol. **28**:590–599.
8. **Crawford, L., K. Leppard, D. Lane, and E. Harlow.** 1982. Cellular proteins reactive with monoclonal antibodies directed against simian virus 40 T-antigen. J. Virol. **42**:612–620.
9. **DeRobertis, E. M., and J. E. Mertz.** 1977. Coupled transcription-translation of DNA injected into *Xenopus* oocytes. Cell **12**:175–182.
10. **DeRobertis, E. M., and M. V. Olson.** 1979. Transcription and processing of cloned yeast tyrosine tRNA genes microinjected into frog oocytes. Nature (London) **278**:137–143.
11. **Dolecki, G. J., and L. D. Smith.** 1979. Poly (A)$^+$ RNA metabolism during oogenesis in *Xenopus laevis*. Develop. Biol. **69**:217–236.
12. **Fitzgerald, M., and T. Shenk.** 1981. The sequence 5′-AAUAAA-3′ forms part of the recognition site for polyadenylation of late SV40 mRNAs. Cell **24**:251–260.
13. **Ford, J. P., and M.-T. Hsu.** 1978. Transcription pattern of in vivo-labeled late simian virus 40 RNA: equimolar transcription beyond the mRNA 3′ terminus. J. Virol. **28**:795–801.
13a. **Fradin, A., J. L. Manley, and C. L. Prives.** 1982. Methylation of simian virus 40 *Hpa*II site affects late, but not early, viral gene expression. Proc. Natl. Acad. Sci. U.S.A. **79**:5142–5146.
14. **Gurdon, J. B.** 1976. Injected nuclei in frog oocytes: fate, enlargement, and chromatin dispersal. J. Embryol. Exp. Morphol. **36**:523–540.
15. **Gurdon, J. B., and D. D. Brown.** 1978. The transcription of 5S DNA injected into *Xenopus* oocytes. Develop. Biol. **67**:346–356.
16. **Gurdon, J. B., and D. A. Melton.** 1981. Gene transfer in amphibian eggs and oocytes. Annu. Rev. Genet. **15**:189–218.
17. **Harland, R. M., and R. A. Laskey.** 1980. Regulated replication of DNA microinjected into eggs of *Xenopus laevis*. Cell **21**:761–771.
18. **Hay, N., H. Skolnik-David, and Y. Aloni.** 1982. Attenuation in the control of SV40 gene expression. Cell **29**:183–193.
19. **Kressmann, A., S. G. Clarkson, V. Pirrotta, and M. L. Birnstiel.** 1978. Transcription of cloned tRNA gene fragments and subfragments injected into the oocyte nucleus of *Xenopus laevis*. Proc. Natl. Acad. Sci. U.S.A. **75**:1176–1180.
20. **Laskey, R. A., B. M. Honda, A. D. Mills, N. R. Morris, A. H. Wyllie, J. E. Mertz, E. M. DeRobertis, and J. B. Gurdon.** 1978. Chromatin assembly and transcription in eggs and oocytes of *Xenopus laevis*. Cold Spring Harbor Symp. Quant. Biol. **42**:171–178.
21. **Lebowitz, P., and S. Weissman.** 1979. Organization and transcription of the simian virus 40 genome. Curr. Top. Microbiol. Immunol. **87**:43–172.
22. **Melton, D. A., and R. Cortese.** 1979. Transcription of cloned tRNA genes and the nuclear partitioning of a tRNA precursor. Cell **18**:1165–1172.
23. **Mertz, J. E.** 1982. Linear DNA does not form chromatin containing regularly spaced nucleosomes. Mol. Cell. Biol. **2**:1608–1618.
24. **Mertz, J. E., and J. B. Gurdon.** 1977. Purified DNAs are transcribed after microinjection into *Xenopus* oocytes. Proc. Natl. Acad. Sci. U.S.A. **74**:1502–1506.

25. **Miller, T. J., and J. E. Mertz.** 1982. Template structural requirements for transcription in vivo by RNA polymerase II. Mol. Cell. Biol. **2**:1595–1607.
26. **Probst, E., A. Kressmann, and M. L. Birnstiel.** 1979. Expression of sea urchin histone genes in the oocyte of *Xenopus laevis*. J. Mol. Biol. **135**:709–732.
27. **Raskas, H. J., and M. Green.** 1971. DNA-RNA and DNA-DNA hybridization in virus research, p. 247–269. *In* K. Maramorosch and H. Koprowski (ed.), Methods in virology, vol 5. Academic Press, Inc., New York.
28. **Rigby, P. W. J., M. Dieckmann, C. Rhodes, and P. Berg.** 1977. Labeling deoxyribonucleic acid to high specific activity *in vitro* by nick translation with DNA polymerase I. J. Mol. Biol. **113**:237–251.
29. **Rosbash, M., and P. J. Ford.** 1974. Polyadenylic acid-containing RNA in *Xenopus laevis* oocytes. J. Mol. Biol. **85**:87–101.
30. **Rungger, D., J. P. Huber, and H. Türler.** 1979. SV40 DNA injected into *Xenopus* oocytes nuclei is transcribed by RNA polymerase B. Cell Biol. Int. Rep. **3**:183–188.
31. **Rungger, D., and H. Tüler.** 1978. DNAs of simian virus 40 and polyoma direct the synthesis of viral tumor antigens and capsid proteins in *Xenopus* oocytes. Proc. Natl. Acad. Sci. U.S.A. **75**:6073–6077.
32. **Stephens, D. L., T. J. Miller, L. Silver, D. Zipser, and J. E. Mertz.** 1981. Easy-to-use equipment for the accurate microinjection of nanoliter volumes into the nuclei of amphibian oocytes. Anal. Biochem. **114**:299–309.
33. **Southern, E. M.** 1975. Detection of specific sequences among DNA fragments separated by gel electrophoresis. J. Mol. Biol. **98**:503–517.
34. **Tegtmeyer, P., and B. Andersen.** 1981. Partial purification of SV40 A protein and a related cellular protein from permissive cells. Virology **115**:67–74.
35. **Thomas, P. S.** 1980. Hybridization of denatured RNA and small DNA fragments transferred to nitrocellulose. Proc. Natl. Acad. Sci. U.S.A. **77**:5201–5205.
36. **Tooze, J. (ed.).** 1980. DNA tumor viruses. Molecular biology of tumor viruses, 2nd ed., part 2. Cold Spring Harbor Laboratory, Cold Spring Harbor, N.Y.
37. **Wickens, M. P., S. Woo, B. W. O'Malley, and J. B. Gurdon.** 1980. Expression of a chicken chromosomal ovalbumin gene injected into frog oocyte nuclei. Nature (London) **285**:628–634.